Analysis of noncircular fluid-filled boreholes in elastic formations using a perturbation model

Ergün Şimşek and Bikash K. Sinha[a)]
Schlumberger-Doll Research, 1 Hampshire Street, Cambridge, Massachusetts 02139

(Received 16 November 2007; revised 11 March 2008; accepted 23 April 2008)

This paper presents a perturbation model to obtain flexural mode dispersions of noncircular fluid-filled boreholes in homogeneous elastic formations. The perturbation model is based on Hamilton's principle with a modified procedure for the reference state selection in order to handle the directional sensitivity of the flexural modes. The accuracy of the perturbation model has been confirmed by comparison to boundary integral solutions. Numerical results confirm that for a fast formation, even modes, and for a slow formation, odd modes are more sensitive to changes in the borehole elongation and azimuth. Even though the focus of this work is on elliptical boreholes and breakouts, the formulation is valid for any kind of noncircular borehole.
 [DOI: 10.1121/1.2931954]

PACS number(s): 43.40.Ph, 43.20.Bi, 43.20.Ks, 43.20.Mv [RAS] Pages: 213–217

I. INTRODUCTION

Borehole cross section affects the propagation of guided modes, such as the lowest-order axisymmetric Stoneley, flexural, and quadrupole modes. Breakouts, which are commonly encountered during underbalance drilling in the presence of large tectonic stresses, can cause complex perturbations to the borehole cross section. The influence of breakouts on the borehole Stoneley, flexural, and quadrupole dispersions has been studied by using finite-difference time domain (FDTD),[1] finite element,[2] and boundary integral equations (BIEs).[3] Since the breakout azimuth coincides with the minimum horizontal stress direction, the distorted borehole cross section can be used to estimate the maximum horizontal stress magnitude.[4–7] Ellefsen *et al.*[8] have also presented a perturbation model (PM) for analyzing modes in noncircular boreholes in anisotropic formations. However, computational results for noncircular boreholes are described only for axisymmetric tube waves.

It has been indicated that the presence of a symmetric breakout causes the flexural wave splittings in the intermediate frequency band similar to the case of an elliptical hole. The two canonical dispersions in a fast formation approximately correspond to the largest and smallest diameters of the distorted borehole cross section.[1] When the influence of breakouts on borehole dispersions is obtained by using FDTD formulation, small changes in the borehole elongation or angular spread are not distinguished very easily. However, such small changes in the borehole cross section can be identified by monitoring perturbations in the guided mode dispersions from a reference circular borehole case. Hence, to understand the effect of breakouts on borehole dispersions, we develop a PM based on Hamilton's principle, which is more sensitive than FDTD. A PM relates fractional changes in the harmonic frequency to fractional changes in the model parameters for a fixed propagation constant. In addition, we analyze the effects of noncircular boreholes on flexural dispersions by using a BIE solver. In other words, we use two different approaches (PM and BIE) to analyze elliptical boreholes and symmetric breakouts that lead to splitting of flexural waves into two canonical waves which are largely sensitive to the long and short diameters of the distorted borehole.

We describe an appropriate method for the selection of reference state for the PM to minimize the difference between perturbed and reference states. We compare results obtained from these two different approaches for both fast and slow formations. Both methods confirm that flexural modes split into two distinct branches (odd and even modes) according to radial polarization parallel to the minor and major axes of the borehole.

The organization of this paper is as follows. In the first section, we briefly describe the implementation of variational principle to the case of a noncircular borehole and a selection procedure for a reference state for even and odd modes. We review a boundary integral formulation and present some illustrative examples. In the second section, we present numerical results obtained from these two different approaches and compare their sensitivity to borehole elongation/breakout azimuth to show the accuracy of the model. Finally, some conclusions are provided.

II. THEORY

In this work, we use two different numerical techniques to analyze noncircular boreholes: a PM and a BIE solver.

Different ways of deriving PMs for elastodynamic problems have been reported.[8–11] In this work, we follow a PM developed by Sinha[12] based on Hamilton's principle that conveniently predicts changes in dispersion curves due to small alterations in either borehole cross section or any of the six fundamental material parameters of the borehole model (borehole fluid mass density ρ_f, fluid compression modulus λ_f, formation mass density ρ, formation elastic moduli λ and μ, and borehole radius a).

[a)]Electronic mail: sinha1@slb.com

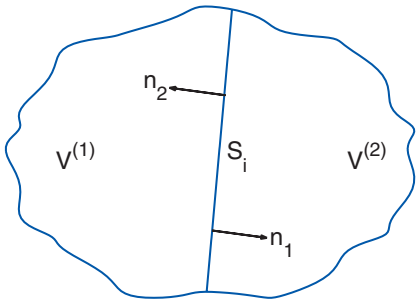

FIG. 1. Outward surface normal n_i is defined on internal surface of discontinuity S_i which is a fluid-solid boundary.

To deal with noncircular boreholes or effects of altered borehole diameter on modal propagation, we express perturbations in the harmonic frequency $\Delta\omega$ and wavenumber Δk_z in terms of the following integrals:[12]

$$\Delta k_z \int_V dV e_{ij} c_{ijkl} e_{kl} - \Delta\omega \int_V dV \rho\omega u_j u_j = \frac{1}{2}\int_V dV(\omega^2 u_j u_j \Delta\rho - e_{ij}\Delta c_{ijkl} e_{kl}) + \int_{S_i} dS[n_i \tau_{ij} \Delta u_j]_{(1)}^{(2)}, \tag{1}$$

where the surface normal is n_i and the Lagrangian energy density in a volume V is expressed as a functional of displacements associated with the wave solution u_j, harmonic frequency ω, wavenumber k_z, elastic moduli c_{ijkl}, mass density ρ, stress tensor elements $\tau_{ij}=c_{ijkl}u_{l,k}$, associated strains $e_{ij}=0.5(u_{i,j}+u_{j,i})$, and locations of interfaces or internal surfaces of discontinuity S_i. We have used a Cartesian tensor notation, and the convention that a comma followed by an index j denotes differentiation with respect to x_j. The summation convention for repeated tensor indices is also implied. The integral on an internal surface of discontinuity S_i between $V^{(1)}$ and $V^{(2)}$ is calculated in terms of outward surface normal n_i, as shown in Fig. 1. Note that the unperturbed cross section corresponds to a circular borehole whose solution is known.

Since the displacement and traction are continuous at a solid-solid interface, and only normal components of the displacements and traction are continuous at a fluid-solid interface, the resulting perturbation in the harmonic frequency ω can be calculated for a fixed wavenumber k_z as follows:

$$\Delta\omega \int_V dV \rho\omega u_j u_j = \frac{1}{2}\int_V dV(\Delta c_{ijkl} e_{kl} e_{ij} - \omega^2 \Delta\rho u_i u_i) + \int_{S_i} dS[h n_i \tau_{ij} n_k u_{j,k}]_{(1)}^{(2)} - \int_{S_i} dS(h_{,j} - n_j n_l h_{,l})[u_j n_k n_i \tau_{ki}]_{(1)}^{(2)}, \tag{2}$$

where h is the radial displacement along n_i and $h_{,i}$ denotes change in the normal between the perturbed and unperturbed interfaces.

For each value of the axial wavenumber k_z, the unperturbed modal eigenfunction is first obtained. Then the integrals in Eq. (2) are performed to obtain the frequency perturbation $\Delta\omega$. These are added to the eigenfrequency ω for various values of k_z to obtain the final dispersion curves for the perturbed case.

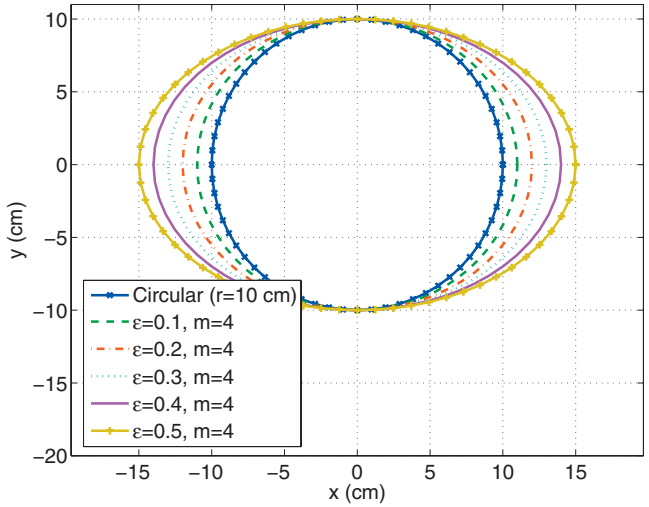

FIG. 2. Noncircular borehole examples for fixed m and changing ϵ.

Phase slowness dispersions can be readily obtained by expressing the slowness perturbation in terms of the frequency perturbation at a given wavenumber. Let the unperturbed modal phase slowness be S_0 and the actual phase slowness be $S=(S_0+\varepsilon\Delta S)$ at a given wavenumber k_z. Then

$$k_z = \omega S = (\omega + \varepsilon\Delta\omega)(S_0 + \varepsilon\Delta S), \tag{3}$$

which yields the following relationship between the slowness and frequency perturbations at a given wavenumber:

$$\Delta S = -\frac{S}{\omega}\Delta\omega, \tag{4}$$

where terms of order higher than ϵ are neglected.

Closed form expressions for the integrals in the denominator are given in Appendix B of Ref. 11, and closed form expressions are given for the ϕ integration of the flexural wave solution in cylindrical coordinates in Sec. B of Ref. 12.

A major contribution of this work is in modeling of modal dispersions for noncircular boreholes and an optimal selection of reference state. We use the following equation to define elliptical boreholes and breakouts:

$$r_{\rm nc}(\theta) = r_{\rm circ}(1 + \epsilon\cos^m\theta), \tag{5}$$

where $r_{\rm nc}(\theta)$ is the radial distance at an angle θ, $r_{\rm circ}$ is the radius of the circular borehole, ϵ is the borehole elongation, and different angular spreads can be obtained by using different m values. For example, $m=4$ provides a good approximation of an elliptical case as shown in Fig. 2 which depicts five different geometries obtained by using $\epsilon=\{0.1,0.2,0.3,0.4,0.5\}$, $m=4$, and $r_{\rm circ}=10$ cm. Figure 3 shows four different geometries obtained by using $m=\{4,12,24,48\}$ and $\epsilon=0.5$; clearly increasing m decreases the angular spread.

To minimize the difference between the reference and perturbed states, we use a circular borehole with a radius $r_{\rm ref}$ that depends on the shape of noncircular borehole as follows:

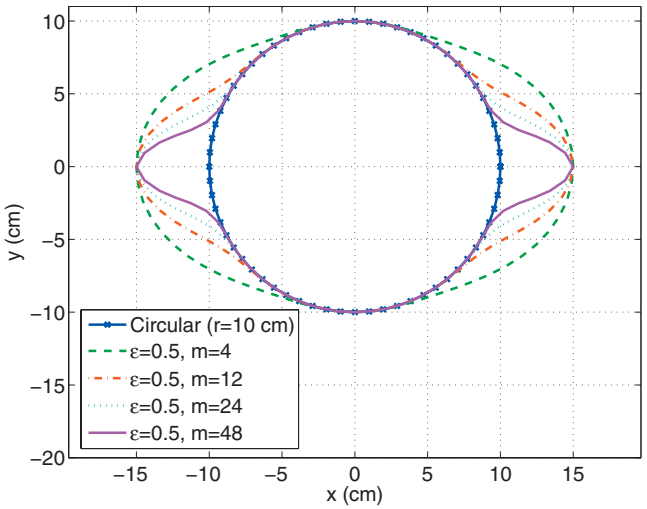

FIG. 3. Noncircular borehole examples for fixed ϵ and changing m.

$$r_{\text{ref}}^{\text{fast,even}} = r_{\text{ref}}^{\text{slow,odd}} = \frac{\int r_{\text{nc}}(\theta)\cos^n \theta d\theta}{\int \cos^n \theta d\theta},$$

$$r_{\text{ref}}^{\text{fast,odd}} = r_{\text{ref}}^{\text{slow,even}} = \frac{\int r_{\text{nc}}(\theta)\sin^n \theta d\theta}{\int \sin^n \theta d\theta}, \tag{6}$$

where n is a parameter appropriately selected for even and odd modes. Equation (6) clearly indicates that borehole radius in the reference state is sensitive to radial polarization direction. Based on our simulation results, we obtain optimum values for n, which are $n=6$ for even modes and $n=2$ for odd modes for a fast formation, and $n=2$ for even modes and $n=6$ for odd modes for a slow formaiton. Figure 4 shows the radius of the reference state for different m values for $\epsilon=0.5$.

Another approach for obtaining modal dispersions of noncircular boreholes is to solve a BIE.[3] In this method, the displacement and stresses on the borehole wall are expressed as integrals over a surface distribution of effective sources, in the frequency-axial wave number (ω-k_z) domain. The unknown sources are approximated by sums of finite basis functions, which are then determined by enforcing boundary

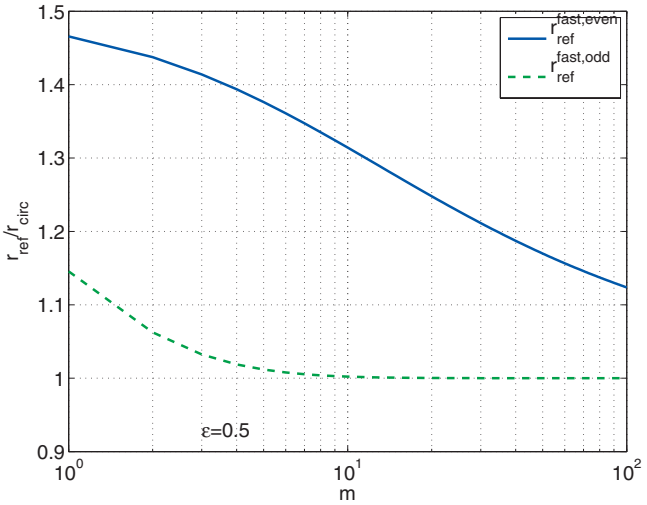

FIG. 4. The radius of the reference state vs m for even and odd modes.

TABLE I. Formation and borehole fluid properties.

Formation	V_P (km/s)	V_S (km/s)	ρ (g/cm^3)
Fast	4.848	2.601	2.16
Slow	2.545	1.018	2.00
Fluid	1.5	⋯	1.0

conditions. The discretized equations form a homogeneous system whose determinant vanishes when (ω-k_z) correspond to a nontrivial solution for the mode of interest.

Again, we have four boundary conditions: the continuity of normal displacement, the continuity of normal stress, the vanishment of the radial-axial stress, and the vanishment of the radial-hoop stress at the solid/liquid boundary. These conditions can be written as

$$\int_C [\hat{\mathbf{n}}(s)\cdot G_u^l(s,s')\mathbf{f}^l(s') - \hat{\mathbf{n}}(s)\cdot G_{uf}^l(s,s')Q(s')]ds' = 0, \tag{7}$$

$$\int_C [\hat{\mathbf{n}}(s)\cdot G_\tau^l(s,s')\mathbf{f}^l(s') - G_{\tau f}^l(s,s')Q(s')]ds' = 0, \tag{8}$$

$$\int_C \hat{\mathbf{s}}(s)\cdot G_\tau^l(s,s')\mathbf{f}^l(s')ds' = 0, \tag{9}$$

$$\int_C \hat{\mathbf{z}}(s)\cdot G_\tau^l(s,s')\mathbf{f}^l(s')ds' = 0, \tag{10}$$

where $\mathbf{f}$ and Q are the distribution of forces and sources, respectively, over the borehole surface S and $G_\eta^l(s,s')$'s are transformed Green's tensors.[3] To solve above equations numerically, we approximate the unknowns ($\mathbf{f}^l$ and Q) by sums of triangular basis functions, remove the integrable singularities, and calculate their contribution analytically. The remaining smooth functions are integrated by a third-order Gaussian quadrature.

Note that a typical "mode-search" routine requires evaluation of the above integrals for $N_f \times N_V$ times, where N_f is the number of the frequency samples of interest and N_V is the number of the velocity samples to calculate the determinants. By analyzing the sign changes in these determinant values, we roughly know where the root is. A simple interpolation technique can provide us more accurate estimate of the root location. Higher N_V value gives more accurate and more smoother results but it requires more computation time. The interpolation and low N_V might create some oscillations in the final result.

III. NUMERICAL RESULTS

To check the accuracy of our PM, we conduct two sets of numerical experiments: one with a fast formation and one with a slow formation. The properties of these formations are presented in Table I.

For each numerical experiment, we first analyze elliptical boreholes, then borehole breakouts for even and odd modes separately. The radius of the circular borehole in Eq.

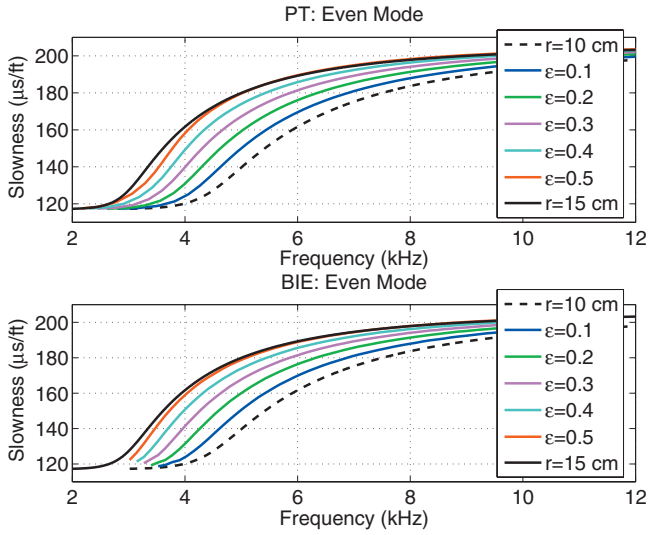

FIG. 5. *Fast formation, even modes, fixed m, and changing* ϵ: Dispersion curves obtained by two different approaches: PT (top) and BIE (bottom), $r_{\text{circle}}=10$ cm, $m=4$, $\epsilon=\{0.1,0.2,0.3,0.4,0.5\}$.

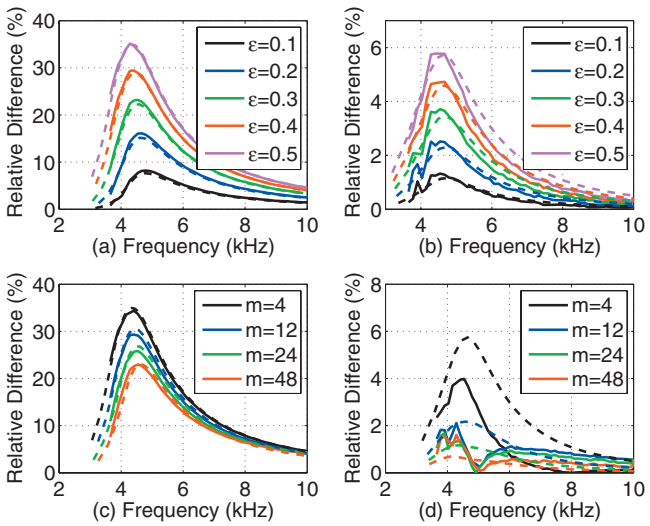

FIG. 6. *Fast formation: sensitivity analysis using two different approaches: PT (lines) and BIE (dashed lines).* (a) Even mode for $m=4$ and changing ϵ, (b) odd mode for $m=4$ and changing ϵ, (c) even mode for $\epsilon=0.5$ and changing m, and (d) odd mode for $\epsilon=0.5$ and changing m.

(5) is 10 cm, and then we generate five different elliptical boreholes using $\epsilon=\{0.1,0.2,0.3,0.4,0.5\}$ for $m=4$, shown in Fig. 2. To mimic breakouts, we use $m=\{4,12,24,48\}$ for $\epsilon=0.5$, shown in Fig. 3. We obtain dispersion curves for each case separately. For example, Fig. 5 shows even mode dispersions obtained by a perturbation theory (PT) and BIE for five different elliptical boreholes. Clearly, the dispersion curves obtained from the PT and BIE methods agree well with each other.

However, sometimes it is not easy to distinguish differences between dispersions due to small changes in the borehole elongation or angular spread. To make the comparison easier, we plot relative slowness difference (ΔS) between the dispersion curve of a noncircular borehole (S_{nc}) and a corresponding reference dispersion of a circular borehole (S_{c}) with $r=r_{\text{minor}}$, such as

$$\Delta S = \left| \frac{S_{\text{c}} - S_{\text{nc}}}{S_{\text{c}}} \right|. \tag{11}$$

Figure 6 shows sensitivity analyses for a fast formation using two different techniques: PT (regular lines) and BIE (dashed lines). In the top row, we plot the sensitivity of even (a) and odd (b) modes to changes in borehole elongation, whereas the bottom row depicts the sensitivity of even (c) and odd (d) modes to changes in breakout azimuth. Notice that the sensitivity of the odd mode to breakout azimuth could not be evaluated smoothly using BIE due to the interpolation scheme used for the calculation of the modal dispersion. However, the main conclusions of these comparisons are (i) the results obtained with PM agree well with BIE solver results confirming the accuracy of our PM, (ii) even modes are more sensitive than odd modes to changes in borehole elongation/breakout azimuth for a fast formation.

Figure 7 follows the same notation and results for a slow formation (see Table I for the formation properties). Even though the difference between the results of PT and BIE is more significant than the fast formation case, we can still conclude that for a slow formation odd mode is more sensitive to borehole elongation/breakout azimuth than the even mode.

We also analyze the influence of the breakout parameters on the maximum perturbations in slowness dispersions. Figure 8 shows ϵ versus ΔS_{max} in *linear-linear* scale (top row) and m versus ΔS_{max} in *log-linear* scale (bottom row) for the fast and slow formations in the left and right columns, respectively. We can conclude that the maximum perturbation changes linearly with the change in the borehole elongation, whereas there is a logarithmic relationship between m and the maximum perturbation. Again, from Fig. 8 we can conclude that even modes are more sensitive to breakout elongation/azimuth than odd modes in fast formations; in contrast, odd modes are more sensitive to breakout elongation/azimuth than even modes in slow formations.

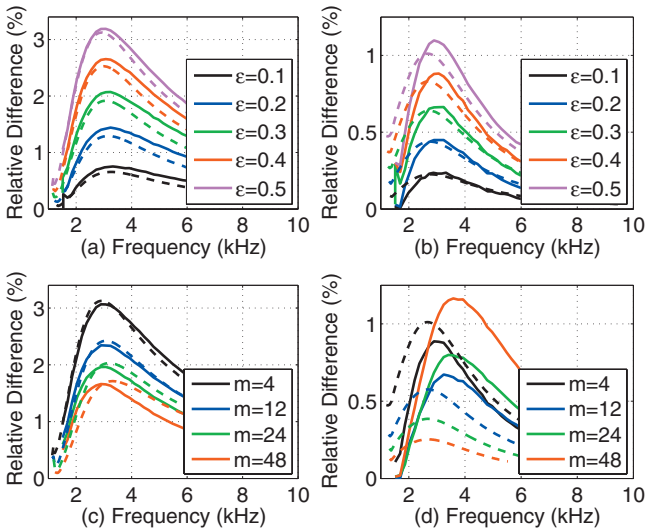

FIG. 7. *Slow formation: sensitivity analysis using two different approaches: PT (lines) and BIE (dashed lines).* (a) Odd mode for $m=4$ and changing ϵ, (b) even mode for $m=4$ and changing ϵ, (c) odd mode for $\epsilon=0.5$ and changing m, and (d) even mode for $\epsilon=0.5$ and changing m.

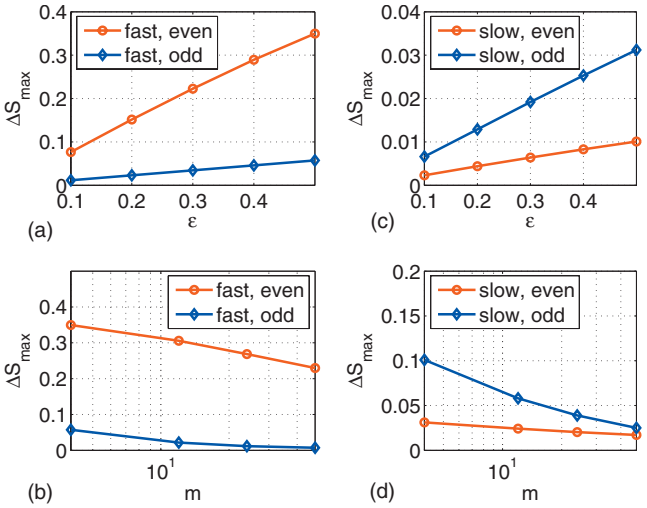

FIG. 8. The influence of the geometry parameters on the maximum perturbations: left column for the fast formation and right column for the slow formation; top row ϵ vs $\Delta S_{\max}$ in *linear-linear* and bottom row m vs $\Delta S_{\max}$ in *log-linear* scale.

We observe that evaluation of boundary integrals at high frequencies becomes less accurate because of a need for an increasingly finer discretization of the geometry. In contrast, a PM is likely to become less accurate with an increasing amount of perturbation from a chosen reference state. We are able to maintain a high degree of accuracy with the PM because of a new technique used for calculating the circular borehole reference state for both the fast and slow formations. Consequently, we find that the PM results are more sensitive to small perturbations in borehole shape than the BIE results.

IV. CONCLUSION

A PM based on Hamilton principle enables us to obtain flexural dispersions of noncircular boreholes in homogeneous elastic formations. We use different reference states depending on borehole elongation and its angular spread for even and odd modes. The accuracy of the method has been validated with a BIE solver. It has been observed that even modes are more sensitive to breakout elongation/azimuth than odd modes in fast formations; whereas odd modes are more sensitive to breakout elongation/azimuth than even modes in slow formations. We have observed that the maximum slowness perturbation from a reference circular borehole exhibits a linear dependence on breakout elongation ϵ and a logarithmic dependence on breakout width parameter m. These can be used for inversion of formation parameters and also as indicators of the presence of breakouts. The results of sensitivity of flexural dispersions to changes in borehole breakout parameters are very similar using either PM or BIE technique. However, numerical results show that our PM is even more sensitive than BIE solution, since in a BIE approach, the modes are obtained via an interpolation technique. Even though we have analyzed elliptical boreholes and breakouts, the formulation is valid for any kind of noncircular borehole.

[1]E. Simsek, B. K. Sinha, S. Zeroug, and N. Bounoua, "Influence of breakouts on borehole sonic dispersions," SEG Technical Program Expanded Abstracts **26**, 313–317 (2007).
[2]L. Nicoletis, A. Bamberger, J. Quiblier, P. Joly, and M. Kern, "Hole geometry and anisotropic effects on tube-wave propagation: A quasi-static study," Geophysics **55**, 167–175 (1990).
[3]C. Randall, "Modes of noncircular fluid-filled boreholes in elastic formations," J. Acoust. Soc. Am. **89**, 1002–1016 (1991).
[4]J. Bell and D. Gough, "The use of borehole breakout in the study of crustal stress," in *Hydraulic Fracturing Stress Measurements*, edited by M. Zoback and B. Haimson (National Academic, Washington, D.C., 1983), pp. 201–209.
[5]M. Zoback, D. Moos, L. Mastin, and R. Anderson, "Wellbore breakouts and in-situ stress," J. Geophys. Res. **90**, 5523–5530 (1985).
[6]L. Vernik and M. Zoback, "Estimation of maximum horizontal principal stress magnitude from stress-induced wellbore breakouts in the cajon pass scientific research borehole," J. Geophys. Res. **97**, 5109–5119 (1992).
[7]S. K. Grandi, R. Rao, X. Huang, and M. N. Toksoz, "In situ stress modelling at a borehole—a case study," SEG Technical Program Expanded Abstracts **22**, 297–300 (2003).
[8]K. Ellefsen, C. Cheng, and M. Toksöz, "Applications of perturbation theory to acoustic logging," J. Geophys. Res. **96**, 537–549 (1991).
[9]B. A. Auld, *Acoustic Fields and Waves in Solids* (Wiley, New York, 1973), vols. 1 and 2.
[10]H. Tiersten and B. Sinha, "A perturbation analysis of the attenuation and dispersion of surface waves," J. Appl. Phys. **49**, 87–95 (1979).
[11]B. Sinha, A. Norris, and S. Chang, "Borehole flexural modes in anisotropic formations," Geophysics **59**, 1037–1052 (1994).
[12]B. Sinha, "Sensitivity and inversion of borehole flexural dispersions for formation parameters," Geophys. J. Int. **128**, 84–96 (1997).